Journal of
Plankton Research

plankt.oxfordjournals.org

J. Plankton Res. (2016) 38(1): 122–130. First published online November 29, 2015 doi:10.1093/plankt/fbv092

Hollow aggregations of moon jellyfish (*Aurelia* spp.)

JAMES H. CHURNSIDE[1]*, RICHARD D. MARCHBANKS[2], PERCY L. DONAGHAY[3], JAMES M. SULLIVAN[4], WILLIAM M. GRAHAM[3] AND R. J. DAVID WELLS[5]

[1]NOAA EARTH SYSTEM RESEARCH LABORATORY, 325 BROADWAY, BOULDER, CO 80304, USA, [2]COOPERATIVE INSTITUTE FOR RESEARCH IN THE ENVIRONMENTAL SCIENCES, NOAA AND UNIVERSITY OF COLORADO, 325 BROADWAY, BOULDER, CO 80304, USA, [3]UNIVERSITY OF SOUTHERN MISSISSIPPI, 1020 BALCH BLVD., STENNIS SPACE CENTER, KILN, MS 39529, USA, [4]FLORIDA ATLANTIC UNIVERSITY - HARBOR BRANCH OCEANOGRAPHIC INSTITUTE, 5600 U.S. 1, FORT PIERCE, FL 34946, USA AND [5]TEXAS A&M UNIVERSITY, 1001 TEXAS CLIPPER RD, OCSB BLDG. 262, GALVESTON, TX 77553, USA

*CORRESPONDING AUTHOR: james.h.churnside@noaa.gov

Received May 11, 2015; accepted October 4, 2015

Corresponding editor: Roger Harris

The relative importance of behavior and currents in forming and maintaining jellyfish aggregations is not completely understood; the objective of this work was to determine how the physical properties of the water column were related to the formation of hollow aggregations of moon jellyfish (*Aurelia* spp.). Hollow aggregations were observed near the surface by airborne lidar in shallow water (<37 m) when the winds were light (<4.3 m s^{-1}). In this work, a hollow aggregation is defined as a region of few individuals surrounded by high densities in the two dimensions defined by depth and the direction of flight. Hydrographic profiles were available for most of the observations, and the bottom of the aggregation was correlated ($R^2 = 0.42$, $P = 8 \times 10^{-4}$) with the depth of the shallow (<13 m) surface mixed layer despite differences in position and time between the lidar observations and the hydrographic measurements. The size and shape of these aggregations suggests that they are not simply a result of advection by local currents, but of active behaviors. A likely mechanism is that the individuals are swimming in a vertical circle, and this behavior is predicted to enhance mixing at the top of the pycnocline.

KEYWORDS: *Aurelia*; moon jellyfish; oceanographic lidar; aerial surveys

INTRODUCTION

The ecological effects of moon jellyfish (*Aurelia* spp.) have been studied extensively (Pauly *et al.*, 2009). While they are responsible for predation on the eggs and larvae of commercially harvested fishes and for competition with the adults for prey (Bailey and Batty, 1983, 1984; Purcell *et al.*, 2000; Purcell and Arai, 2001; Brodeur *et al.*, 2002), they themselves are prey for some animals and provide shelter from predators for others (Zaitsev, 1992; Purcell

© The Author 2015. Published by Oxford University Press. All rights reserved. For permissions, please email: journals.permissions@oup.com

Downloaded from http://plankt.oxfordjournals.org/ by guest on February 1, 2016

and Arai, 2001; Arai *et al.*, 2003; D'ambra *et al.*, 2014). These effects can be magnified locally by 'real' or 'apparent' blooms, which are characterized by rapid population growth or redistribution of a stable population, respectively (Graham *et al.*, 2001). Both real and apparent blooms can produce large aggregations.

There are numerous reports of *Aurelia* forming large aggregations in coastal waters (Hamner and Dawson, 2009; Dong *et al.*, 2010; Crawford *et al.*, 2011). Aggregations in Saanich Inlet, British Columbia, Canada, were observed to form as all animals moved in the same direction when the sun was available for navigation (Hamner *et al.*, 1994). A huge aggregation was reported in the Uwakai Sea, Shikoku, Japan, in 2000, which was formed by an onshore current rather than any behavior of the animals (Uye *et al.*, 2003). Aggregations in Prince William Sound, Alaska, USA, were thought to result from a combination of swimming behavior and local currents (Purcell *et al.*, 2000). Aggregations in Roscoe Bay, British Columbia, Canada, were also a result of the effects of behavior and tidal currents (Albert, 2009). The relative importance of behavior and currents in forming and maintaining these aggregations is not completely understood.

In this paper, we report observations of *Aurelia* aggregations in a shallow fjord in Washington State and in shallow water in the Gulf of Mexico. Airborne lidar was used to measure vertical cross sections of several aggregations, and the results were compared with the physical properties of the water column. The objective of this work was to determine how the physical properties of the water column were related to the formation of hollow aggregations of moon jellyfish.

METHOD

Aggregations of moon jellyfish were observed with the NOAA Fish Lidar, which has been used previously to detect fish schools and plankton layers (Churnside, 2014). The observations were made during two field campaigns, one in May 2009 in East Sound, Orcas Island, Washington State and the other in September 2011 in the Gulf of Mexico.

The lidar has been described in previous publications, but the general characteristics will be repeated here. The lidar transmitter comprised a Q-switched, frequency-doubled, Nd:YAG laser that produced 100 mJ of linearly polarized green (532 nm) light in a 12-ns pulse. The raw laser beam was diverged to produce a 5-m diameter spot on the surface, so that the irradiance at the surface was below that which would cause an ocular hazard for either people or marine mammals (Zorn *et al.*, 2000). Two receivers were used to detect the reflected light; one was sensitive to the same linear polarization as the transmitted light (co-polarized) and the other was sensitive to the orthogonal polarization (cross-polarized). Each receiver comprised a telescope, an aperture at the focus of the primary lens to limit the field of view of the receiver to the divergence of the transmitter, an interference filter (1 nm bandwidth) to limit background light, a photomultiplier tube to convert the collected light into an electrical signal, a logarithmic amplifier to compress the dynamic range of the signal and an 8-bit digitizer sampling at 1 GHz.

Operation of the lidar was similar for both surveys, but there were some differences as a result of the different aircraft that were used. The aircraft for the East Sound survey was a Cessna 177. The small camera port in this aircraft meant that the two receiver channels both used the same size telescope (7 cm diameter) and the system used a fixed pointing angle of 12° off nadir. The limited electrical power available on this aircraft required operation of the laser at a reduced pulse repetition rate of 10 Hz. For the Gulf of Mexico surveys, we used a larger, twin-engine aircraft (Beechcraft King Air 90). Because the camera port was larger, we used a larger cross-polarized receiver telescope (17 cm diameter) to collect more light. It was pointed 15° off nadir to further reduce surface specular reflections in the open waters of the Gulf. Because more electrical power was available, we used the full laser repetition rate of our system (30 Hz). The two aircraft also had different survey speeds, about 40 m s^{-1} over East Sound and 80 m s^{-1} over the Gulf of Mexico, so that a lidar profile was made every 4 m along the flight track in East Sound and every 2.7 m in the Gulf of Mexico. These numbers are only averages, because the speed of the aircraft over the surface varied with the wind speed at the flight altitude of 300 m.

East Sound is ~10 km long and 1–2.5 km wide, with a maximum depth <30 m. Flights were made during daylight hours between 16 May and 26 May 2009, which is a period when temperature stratification of the water column is expected. Winds during this period were generally light, and were <4 m s^{-1} 87% of the time. Each flight comprised non-parallel transects along the length of the sound designed to approximate uniform coverage at each point along the sound despite the varying width. In all, 236 transects were flown in 16 flights. A similar set of flights was made between 8 May and 21 May 2010.

Twenty flights in the northern Gulf of Mexico, including a combination of large- and small-scale patterns, were flown between 24 September and 7 October 2011. This is also a period when stratification of the water column is expected. When possible, a pattern was flown during the day and again the same night, with 43% of the survey time done at night. For 34% of the time, the

Downloaded from http://plankt.oxfordjournals.org/ by guest on February 1, 2016

Fig. 1. Photograph of *Aurelia* aggregation in East Sound taken from the aircraft. The brightest part of the image, where the aggregation is near the surface, is about 25 m long.

surveys were over water <40 m deep. During this period, winds were <4 m s^{-1} 29% of the time.

Multiple factors were used to identify these features as *Aurelia*. All were very close to the surface, so visual identification from the air was possible during the day (e.g. Fig. 1). In East Sound, confirmation was provided by visual identification from the surface vessel and sampling by plankton net. In the Gulf of Mexico, identification at night was based largely on the morphology of the aggregations as determined by the lidar signal. Confirmation was provided by surface trawls. These were generally conducted in deeper water than where the aggregations were found, but caught large numbers of *Aurelia* over a large area of the northern Gulf of Mexico.

Processing of the lidar data was by visual inspection of the cross-polarized data, after referencing each profile to the surface return. Variations in aircraft altitude and attitude produce variations in the distance to the surface, so we found the surface return in each lidar profile and found the depth of each sample based on that and the known speed of light in seawater. The results were displayed as a gray-scale image of the logarithm of the lidar return as a function of depth on the vertical axis and distance along the flight track on the horizontal for 2000 lidar profiles at a time. In this display, the characteristic hollow returns were very obvious. With the mouse, we identified the position in the image of the left side of the aggregation, the right side, the top and the bottom, using the apparent maximum return in each case. The corresponding depths of top and bottom and Global Positioning System (GPS) positions of left and right were saved in a spreadsheet for analysis. The position of the aggregation reported here is that of the center, halfway between the two sides.

For visualization, we also calculated the contrast within each aggregation. First, the attenuation was estimated using the background signal near the aggregation. For each lidar profile, the effect of attenuation was removed using this value. Then the contrast was calculated as

$$C = \frac{S - S_B}{S_B}, \tag{1}$$

where S is the attenuation-corrected signal and S_B is the background value.

In situ density measurements in East Sound were made with a ship-deployed slow-descent high-resolution vertical profiler equipped with a Seabird SBE-25 CTD with a sample rate of 0.17 Hz. Unfortunately, the measurements were not targeted to the jellyfish aggregations, but several profiles were taken each day and the closest was used in the analysis. In some cases, the same profile was used for several aggregations under this criterion. Temperature and salinity were used to calculate potential density. The mean density difference between 15 and 30 m depths for the 30 *in situ* profiles was 0.62 kg m^{-3}, with a standard deviation of 0.24 kg m^{-3}. The high-vertical resolution (1.4 cm) measurements were averaged to 10-cm vertical resolution and the derivative at each depth was estimated from the average over the 20-cm range centered on that depth. The Brunt–Väisälä frequency, BV, is given by

$$\mathrm{BV} = \left(-\frac{g}{\rho}\frac{d\rho}{dz}\right)^{\frac{1}{2}}, \tag{2}$$

where g is the gravitational acceleration, ρ is the potential density and z is the vertical coordinate. The depth of the maximum derivative of potential density is also the depth of maximum BV, and this depth was used to represent the depth of the pycnocline. Oceanographic stations in the Gulf of Mexico were all much farther off shore than the observed aggregations and were not used.

Winds for East Sound were measured at the Orcas Island airport, and were obtained from the Weather Underground website (http://www.wunderground.com). These observations may be different from the winds over the water, but the airport altitude is 9 m and all aggregations were within 10 km of its location. Casual observations of winds over the water (e.g. whitecapping) were consistent with reported winds at takeoff and landing. Winds for the Gulf of Mexico were measured at National Data Buoy Center Buoy 42040 at 29.212N, 88.207W, and were obtained from the National Data Buoy Center website (http://www.ndbc.noaa.gov).

Regression analyses were used to investigate possible relationships between the geometric parameters of the aggregations and the environmental parameters. The significance of the relationships was determined using a

Downloaded from http://plankt.oxfordjournals.org/ by guest on February 1, 2016

two-tailed, *t*-test with a threshold for the probability of the result being due to chance of $P < 0.05$.

Additional data were provided by a hull-mounted Acoustic Doppler Current Profiler (ADCP, Teledyne RDI) operating at 1228.8 kHz. The shallow-draft vessel was allowed to drift through an aggregation of *Aurelia* that was observed visually in the Gulf of Mexico, and the echo intensity was recorded from a minimum depth of 1.5 m to the bottom with a depth resolution of 0.5 m. For our application, the Doppler information was not used.

RESULTS

The primary result of this paper, based on lidar profiles, is the observation that moon jellyfish form hollow aggregations. For our purposes, a hollow aggregation is defined as a region of few or no individuals that is surrounded by high densities in the two dimensions defined by the depth and the direction of flight. This definition translates into a lidar contrast of <0.1 in the central region and of >0.5 in the surrounding region. This surrounding region was usually continuous, but there were gaps in a few of the aggregations. The largest gap covered about a third of the bottom section. The morphology of aggregations of *Aurelia* spp. in the NE Pacific in the Gulf of Mexico was very similar. An example (Fig. 2a, Aggregation 7) clearly shows a lidar return that is at background levels in the center of the aggregation. In all, we observed 33 aggregations, including one that contained two hollow regions (Fig. 2b, Aggregation 23). For 23 of those aggregations, we also had *in situ* profiles of temperature and salinity that were made nearby on the same day.

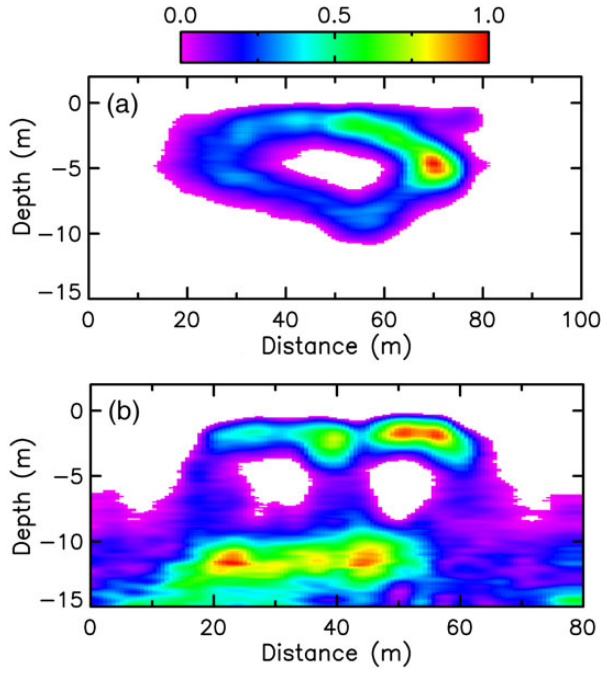

Fig. 2. Lidar return from aggregations of jellyfish (*Aurelia* sp.) as a function of depth and distance along the flight track. Color provides normalized contrast, C/C_{max}, according to the color bar at the top. (**a**) Aggregation 7 in the tables, $C_{max} = 5.4$. (**b**) Aggregation 23, $C_{max} = 3.7$.

Not all of the lidar targets had a hollow shape. In East Sound, there were 107 total detections, of which 24% were hollow. Note that the probability of observing a hollow shape in a lidar pass over a hollow aggregation is given by the ratio of the width of the hollow section to the overall width. For the example of Fig. 2a, this probability is 30%, implying that most of the non-hollow observations could be a result of measurements of the edges of hollow aggregations. If this is the case, the average length of the non-hollow detections across the edges should be less than the average length of the hollow detections across the centers, and the values of 42 m for the non-hollow detections and 54 m for the hollow detections support this. If the non-hollow detections are detections of the edges of hollow aggregations, this suggests that the total number of detections each day and the number of hollow detections on the same day should be highly correlated, and this was the case ($R^2 = 0.87$, $P = 3 \times 10^{-5}$, $N = 11$). These indirect arguments suggest that most, if not all, of the aggregations in East Sound were actually hollow. The situation in the Gulf of Mexico is complicated by the presence of other aggregating species—mostly schooling fishes that were not present in East Sound. Only 3.5% of 228 total detections in the Gulf of Mexico were hollow, but there is no way to infer from the data how many of the non-hollow detections were *Aurelia* aggregations.

The density of the hollow aggregations was not measured directly, but an estimate can be made by comparison with the results of Uye *et al.* (Uye *et al.*, 2003). That paper presented a photograph of aggregations of *Aurelia* in an inlet of the Uwakai Sea taken from the same flight altitude as Fig. 1. While the sizes and shapes of those aggregations are very different from ours, the range of color and contrast are very similar. In both aerial photographs, the ratio of the maximum brightness in the aggregation to that of the surrounding water is about two, suggesting that the density is similar in the two cases. From their *in situ* sample results, we infer that the highest densities in our aggregations are of the order of 100 m^{-3}.

The physical dimensions of the hollow aggregations in Table I show a 5-fold variation in length, from 19 to 100 m. There was a significant ($P = 0.0038$ in a two-tailed *t*-test) difference between the lengths from East Sound (54 ± 23 m) and the Gulf of Mexico (36 ± 9 m). The heights from East Sound (6.6 ± 1.6 m) were not significantly different from the heights in the Gulf of Mexico

Downloaded from http://plankt.oxfordjournals.org/ by guest on February 1, 2016

Table I: Parameters of the observed aggregations and the corresponding environmental parameters where available

Aggr. number	Length (m)	Height (m)	Bottom depth (m)	Water depth (m)	Wind speed (m s^{-1})	Max BV depth (m)
1	29.0	6.21	7.73	<30	2.9	–
2	29.0	7.08	8.06	22	3.5	7.7
3	26.8	6.53	7.73	25	3.6	7.7
4	58.5	7.62	8.82	22	1.0	5.4
5	56.5	5.99	5.99	25	1.2	5.4
6	43.7	3.81	4.14	27	1.2	5.4
7	55.4	4.14	4.79	23	1.2	5.4
8	75.3	7.84	7.95	18	1.2	5.4
9	63.3	5.01	5.34	27	1.2	5.4
10	55.4	4.46	4.57	23	1.2	4.4
11	47.5	5.66	5.88	23	1.2	4.4
12	68.6	5.01	5.45	25	1.5	5.4
13	28.2	3.59	4.14	27	1.5	5.4
14	100.0	6.97	7.08	24	0.9	4.2
15	75.6	6.86	6.86	24	1.1	4.2
16	97.6	8.28	8.28	24	1.4	4.2
17	25.4	4.36	5.77	20	1.8	5.6
18	37.5	7.95	8.60	24	0.5	7.7
19	49.2	8.82	9.26	24	3.2	12.8
20	91.6	7.51	8.60	30	3.2	12.8
21	35.8	8.49	9.26	30	3.2	12.8
22	82.8	9.04	9.91	30	3.3	12.8
23	54.3	6.21	7.30	30	3.3	12.8
24	54.0	7.95	8.60	30	3.1	12.8
25	19.3	7.73	10.13	30	2.7	–
26	39.5	7.30	7.30	30	2.8	–
27	44.0	6.86	8.82	16	0.4	–
28	45.5	7.08	7.30	26	0.2	–
29	22.7	6.32	6.53	25	0.2	–
30	28.3	5.66	6.32	26	0.2	–
31	42.5	6.21	6.75	26	0.2	–
32	38.1	5.23	5.23	37	2.3	–
33	32.5	7.95	8.17	10	4.3	–

Height is the maximum distance from the bottom of the aggregation to the top. The first 24 aggregations were observed in East Sound, all during the day. All of the rest were observed in the Gulf of Mexico, and all were at night except for Aggregation 32. The GPS receiver lost lock when Aggregation 1 was observed, so no position is available.

(6.5 ± 0.9 m). The variation in height is much lower, with values between 3.6 and 9 m. The tops of all aggregations were very close to the surface; the deepest was only 2.4 m and 73% were <1 m from the surface.

The environmental conditions under which the hollow aggregations were observed (Table I) show some interesting characteristics. All of the hollow aggregations were observed in shallow water (≤37 m). Only shallow water was surveyed in East Sound, but most of the survey time was spent beyond the edge of the continental shelf in the Gulf of Mexico. All of the aggregations were observed in light winds (≤4.3 m s^{-1} with an average value of only 1.9 m s^{-1}). The maximum BV was found to be rather shallow (<13 m) for the cases where we had *in situ* density profiles. No pattern with respect to tides was observed; 31% of the observations in East Sound were within 1 h of either a high or low tide, when tidal currents are low.

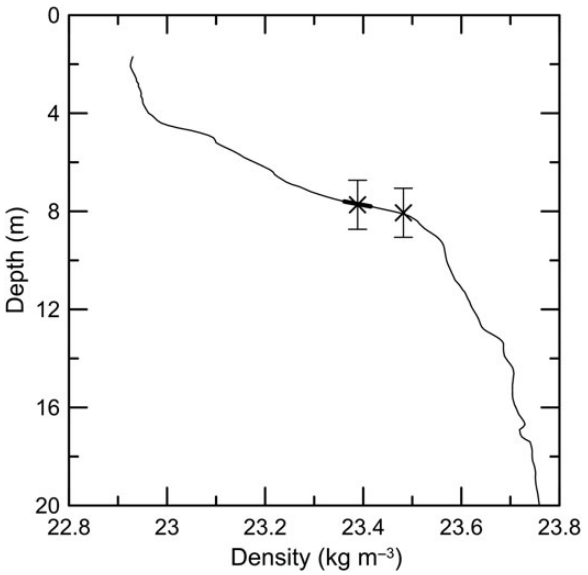

Fig. 3. Smoothed density profile (after subtracting 1000 kg m^{-3}) as a function of depth (thin line), depth of maximum BV (midpoint of thick line) and the range over which it was calculated (thick line) and the bottom depths of the two aggregations associated with this profile (X) with error bars representing the uncertainty in those depths of about 1 m.

Regression analyses between the geometry of the aggregations and the environmental parameters only produced significant correlations between the bottom depth of the aggregation and pycnocline depth ($R^2 = 0.42$, $P = 8 \times 10^{-4}$, $N = 23$). There was also a significant correlation of the bottom depth of the aggregation with wind speed, but wind speed is not an independent predictor; pycnocline depth and wind speed were highly correlated ($R^2 = 0.80$, $P = 9 \times 10^{-9}$, $N = 23$). The average depth of the bottom of the aggregations (7.1 ± 0.5 m) is not significantly different from the average pycnocline depth (7.4 ± 0.7 m). Figure 3 shows the relationship between the first density profile used in the analysis (after averaging to 10-cm vertical resolution) and the bottom depths of the two aggregations that were associated with it (Aggregations 2 and 3).

No acoustic data were found to have the hollow structure seen in the lidar data. As the top of the structure in the lidar data is very close to the surface, one would expect that it would not be present in the acoustic data. As a result, the acoustic data for an initially hollow structure might be expected to look like the example of Fig. 4 in which the evidence of a truncated hollow structure can be seen. The length is similar to the lengths observed by the lidar if the drift speed was just under 1 m s^{-1}, which seems a reasonable value.

Downloaded from http://plankt.oxfordjournals.org/ by guest on February 1, 2016

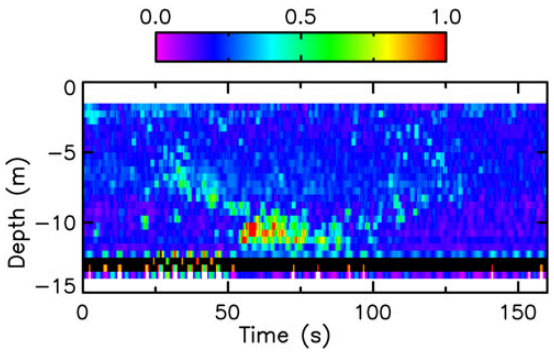

Fig. 4. Acoustic echo from an aggregation of jellyfish (*Aurelia* sp.) as a function of depth and distance along the flight track. Color provides echo intensity, E, normalized by the maximum value in the water column. The black return at about 13 m is the bottom. The color scale was adjusted such that this return is saturated in order to emphasize the water-column features.

DISCUSSION

Most of the hollow aggregations in Table I were seen in East Sound during the day in 2009. No night flights were made over East Sound, however, so they may have also occurred at night. No aggregations were observed in East Sound during the 2010 measurements. During this period, the winds were generally higher (<4 m s^{-1} only 41% of the time). More importantly, very few *Aurelia* were observed. In the Gulf of Mexico, most of the hollow aggregations were made at night. Many fewer hollow aggregations were observed in the Gulf of Mexico than in East Sound, despite the fact that many more hours of data were collected. No aggregations were observed in water deeper than 40 m, even though high numbers of individuals were captured by surface trawls in deeper waters.

There are two possible mechanisms for the formation of the structures we have observed. The first is that the animals are simply drifting with the local currents, which then arrange them in this shape. The other is that they are actively swimming in such a way to produce this shape.

The most obvious physical process by which animals might be aggregated in the observed pattern is Langmuir circulation. The possibility that aggregations of *Aurelia* and other medusae are formed by Langmuir circulation has been considered (Hamner and Schneider, 1986; Larson, 1992; Graham *et al.*, 2001), based on an earlier hypothesis about the influence of Langmuir circulation on the distribution of planktonic crustaceans (Stavn, 1971). While it was not observed, this current pattern could produce a distribution of individuals concentrated around the edge of the circulation. Previous observations were generally under higher winds than in our case, where the horizontal spacing of a typical aggregation is too large compared with the predicted Langmuir cell width. If we assume that the phase speed of the primary surface wave is equal to the wind speed and use the deep-water approximation to the phase speed, we can get an estimate for the wavelength of the surface wave given by Kinsman (Kinsman, 1984)

$$\lambda = \frac{2\pi U^2}{g}, \tag{3}$$

where U is the wind speed and g is the gravitational acceleration. Only one combination of wind speed and water depth violates the conditions for deep water, and this case will be neglected in the analysis. An empirical relation for the width, d, of a Langmuir circulation cell is based on this wavelength and water depth H (Leibovich, 1983):

$$d = 4.8H\left[1 - \exp\left(-\frac{\lambda}{2H}\right)\right]. \tag{4}$$

Values for d range from <1 m to a maximum of 18 m, and are all less than the length of the corresponding aggregation. In the example of Fig. 1, the surface waves and the aggregation are both visible. In this case, the length of the aggregation is about 20λ, while Equation (2) predicts that it should be about 2.4λ. On average, the length of the aggregation is $93d$, and we conclude that Langmuir circulation is not responsible for hollow aggregations of jellyfish. A more precise model for Langmuir circulation could be used, but the scales are so different that this simple model is sufficient to demonstrate that Langmuir cells are not the explanation for the observed aggregations.

Another physical process known to create patches of plankton is internal waves (Lennert-Cody and Franks, 1999; Lai *et al.*, 2010; Macias *et al.*, 2010). These produce circulating currents that might produce the observed shape, although that shape has not been observed in studies of plankton/internal wave interactions. During the period of our observations in East Sound, the water column was strongly stratified and would support internal wave propagation. However, internal waves, if they were present at the time, would have been observed in the lidar data (Churnside and Ostrovsky, 2005; Churnside and Donaghay, 2009; Churnside *et al.*, 2012). None were observed, and we conclude that internal waves were not responsible for the observed aggregations.

The final possibility for aggregation by physical processes requires convergent currents. We note that the currents above the pycnocline in East Sound are driven by the winds, while those below are tidally forced (Dekshenieks *et al.*, 2001). For winds below 4 m s^{-1}, we would expect wind-driven surface currents to be less than $\sim$2% of this, or 0.08 m s^{-1}. This is similar to surface currents measured

Downloaded from http://plankt.oxfordjournals.org/ by guest on February 1, 2016

in the area (Dekshenieks *et al.*, 2001), and we would not expect these small currents to lead to significant convergence. Convergence resulting from shear between the surface layer and deeper tidal currents may produce convergence, but the observations were made at various points in the tidal cycle, so this cannot be the entire explanation. The possibility does exist that some interaction of these processes results in the closed circulation pattern observed, but this seems unlikely, because the patterns in East Sound and the Gulf of Mexico are so similar.

The most direct evidence for a behavioral mechanism comes from a comparison of our observations with video observations by Purcell et al. (Purcell *et al.* 2000). A 3-min drift through their Aggregation 1 at a constant depth of 4.3 m revealed '1 side where medusa were swimming downwards in high (46%) relative density, a central region where medusa were in mixed orientations and low (7%) relative density, and the opposite side where medusa were swimming upwards in high (22%) relative density.' This density pattern is precisely what one would observe drifting though the aggregation of Fig. 2a at that depth. Drift speed was not reported by Purcell *et al.*, but a comparison of Fig. 8 in that paper with Fig. 2a would suggest a speed of around 0.5 m s^{-1}, which is reasonable. This observation of animals swimming upward on one side and downward on the other suggests a closed circulation such as we have observed; if the pattern is to persist for more than a few minutes, animals must be moving from the top of the upward-swimming column to the top of the downward-swimming column and back from the bottom of the downward-swimming column to the bottom of the upward-swimming column. Furthermore, Aggregation 2 in Purcell *et al.* is described as a dense central region of upward-swimming individuals that spreads horizontally at the surface and turns downward at the outer edges of the aggregation. A vertical slice through the density pattern produced by this behavior would look very similar to the example in Fig. 2b.

While it seems unlikely that local currents alone could produce the results we observed, these currents may provide behavioral cues. *Aurelia* have been observed diving to avoid turbulent water (Albert, 2007, 2011). Similar behavior has been observed in other gelatinous animals that avoided the turbulence produced by surface waves or current shear (Miller, 1974; Shanks and Graham, 1987; Graham *et al.*, 2001). In the Gulf of Mexico, *Aurelia* have been observed swimming horizontally where there is a vertical gradient of horizontal current (Rakow and Graham, 2006). *Rhizostoma octopus* have been observed swimming into the local current in order to maintain aggregation (Fossette *et al.*, 2015). Currents were not reported, but Larson (1992) observed *Linuche unguiculata* swimming in horizontal circles. This behavior was only observed in low wind speeds (<4 m s^{-1}). The conclusion of that study was that circular swimming served to maintain the aggregations in low wind speeds. A vertical orbital motion would have the same effect. For spawning populations, the ability to maintain an aggregation in shallow water would increase fertilization success and recruitment (Hamner *et al.*, 1994; Uye *et al.*, 2003).

We note that a circular swimming behavior may also contribute to vertical mixing, at least locally. Estimates of global mixing in the ocean by vertically migrating species, including copepods, euphausiids and some species of gelatinous zooplankton suggest that the effect may be of the same order as mixing by winds and tides (Dewar *et al.*, 2006; Katija, 2012). Locally, motion of zooplankton swarms will increase turbulent mixing (Kunze *et al.*, 2006; Dabiri, 2010) and also induce a drift current in the direction of motion (Katija and Dabiri, 2009; Leshansky and Pismen, 2010). Dabiri (2010) calculated the motion of water induced by a column of rising spheres, concluding that the displacement of the water would be 0.04–0.05 times the displacement of the spheres. This calculation neglected viscosity, and the author noted that the actual displacement of the water would be larger. Katija and Dabiri (2009) published the displacement of a dye patch after passage of a medusa. Examination of Fig. 3 of that paper shows the dye moving 0.11 times the displacement of the animal. We conclude that the circular swimming pattern could induce a circular current of the order of 10% of the swimming speed. Measured swimming speeds are in the range of 1–5 cm s^{-1} (Daniel, 1985; McHenry and Jed, 2003; Gemmell *et al.*, 2013), so the induced currents would be a few mm s^{-1}. Since the bottom of the aggregation enters the top of the pycnocline, this current and the associated turbulence will mix surface water into the pycnocline.

To summarize, we found that *Aurelia* spp. form hollow aggregations near the surface in shallow water ($\leq$37 m) in light winds ($\leq$4.3 m s^{-1}), both during the day and at night. The depth of the bottom of these aggregations is highly correlated with the depth of the pycnocline. The horizontal extent cannot be explained by entrapment in Langmuir circulation cells as some have suggested. Instead, it appears to be a result of individuals swimming in an orbital pattern in order to maintain the cohesion of the aggregation. This orbital motion is constrained by the surface and the pycnocline, and it seems likely that current shear and turbulence provide cues for swimming direction. At the bottom of the aggregation, this behavior will induce currents estimated to be on the order of mm s^{-1} that may lead to erosion of the top of the pycnocline.

Downloaded from http://plankt.oxfordjournals.org/ by guest on February 1, 2016

FUNDING

The East Sound work was partially supported by the Office of Naval Research under grants N0001410IP20035 and N000140811217. Our pilot was Jay Palmer. The Gulf of Mexico work was partially supported by the Natural Resource Damage Assessment program associated with the Deepwater Horizon event. Our pilots were Paolo Ramella and Steve Hederstedt.

REFERENCES

Albert, D. J. (2007) *Aurelia labiata* medusae (Scyphozoa) in Roscoe Bay avoid tidal dispersion by vertical migration. *J. Sea Res.*, **57**, 281–287.

Albert, D. J. (2009) *Aurelia labiata* (Scyphozoa) jellyfish in Roscoe Bay: their spatial distribution varies with population size and their behaviour changes with water depth. *J. Sea Res.*, **61**, 140–143.

Albert, D. J. (2011) What's on the mind of a jellyfish? A review of behavioural observations on Aurelia sp. jellyfish. *Neurosci. Biobehav. Rev.*, **35**, 474–482.

Arai, M. N., Welch, D. W., Dunsmuir, A. L., Jacobs, M. C. and Ladouceur, A. R. (2003) Digestion of pelagic Ctenophora and Cnidaria by fish. *Can. J. Fish. Aquat. Sci.*, **60**, 825–829.

Bailey, K. M. and Batty, R. S. (1983) A laboratory study of predation by *Aurelia aurita* on larval herring (*Clupea harengus*): experimental observations compared with model predictions. *Mar. Biol.*, **72**, 295–301.

Bailey, K. M. and Batty, R. S. (1984) Laboratory study of predation by *Aurelia aurita* on larvae of cod, flounder, plaice and herring: development and vulnerability to capture. *Mar. Biol.*, **83**, 287–291.

Brodeur, R. D., Sugisaki, H. and Hunt, G. L. Jr (2002) Increases in jellyfish biomass in the Bering Sea: implications for the ecosystem. *Mar. Ecol. Prog. Ser.*, **233**, 89–103.

Churnside, J. H. (2014) Review of profiling oceanographic lidar. *Opt. Eng*, **53**, 051405.

Churnside, J. H. and Donaghay, P. L. (2009) Thin scattering layers observed by airborne lidar. *ICES J. Mar. Sci.*, **66**, 778–789.

Churnside, J. H., Marchbanks, R. D., Lee, J. H., Shaw, J. A., Weidemann, A. and Donaghay, P. L. (2012) Airborne lidar detection and characterization of internal waves in a shallow fjord. *J. Appl. Remote Sens.*, **6**, 1–15.

Churnside, J. H. and Ostrovsky, L. A. (2005) Lidar observation of a strongly nonlinear internal wave train in the Gulf of Alaska. *Int. J. Remote Sens.*, **26**, 167–177.

Crawford, C. M., Moltschaniwskyj, N. A. and Wilcox, S. (2011) Size and characteristics of aggregations of moon jellyfish (*Aurelia sp.*) in Tasmania, Australia. *Proc. Royal Soc. Tasmania*, **145**, 9–15.

Dabiri, J. O. (2010) Role of vertical migration in biogenic ocean mixing. *Geophys. Res. Lett.*, **37**, L11602.

D'ambra, I., Graham, W. M., Carmichael, R. H. and Hernandez, F. J. Jr (2014) Fish rely on scyphozoan hosts as a primary food source: evidence from stable isotope analysis. *Mar. Biol.*, **162**, 1–6.

Daniel, T. (1985) Cost of locomotion: unsteady medusan swimming. *J. Exp. Biol.*, **119**, 149–164.

Dekshenieks, M. M., Donaghay, P. L., Sullivan, J. M., Rines, J. E. B., Osborn, T. R. and Twardowski, M. S. (2001) Temporal and spatial occurrence of thin phytoplankton layers in relation to physical processes. *Mar. Ecol. Prog. Ser.*, **223**, 61–71.

Dewar, W. K., Bingham, R. J., Iverson, R. L., Nowacek, D. P., St Laurent, L. C. and Wiebe, P. H. (2006) Does the marine biosphere mix the ocean? *J. Mar. Res.*, **64**, 541–561.

Dong, Z., Liu, D. and Keesing, J. K. (2010) Jellyfish blooms in China: dominant species, causes and consequences. *Mar. Pollut. Bull.*, **60**, 954–963.

Fossette, S., Gleiss, A. C., Chalumeau, J., Bastian, T., Armstrong, C. D., Vandenabeele, S., Karpytchev, M. and Hays, G. C. (2015) Current-oriented swimming by jellyfish and its role in bloom maintenance. *Curr. Biol.*, **25**, 342–347.

Gemmell, B. J., Costello, J. H., Colin, S. P., Stewart, C. J., Dabiri, J. O., Tafti, D. and Priya, S. (2013) Passive energy recapture in jellyfish contributes to propulsive advantage over other metazoans. *Proc. Natl. Acad. Sci. USA*, **110**, 17904–17909.

Graham, W., Pagès, F. and Hamner, W. (2001) A physical context for gelatinous zooplankton aggregations: a review. *Hydrobiologia*, **451**, 199–212.

Hamner, W. and Dawson, M. (2009) A review and synthesis on the systematics and evolution of jellyfish blooms: advantageous aggregations and adaptive assemblages. *Hydrobiologia*, **616**, 161–191.

Hamner, W. M., Hamner, P. P. and Strand, S. W. (1994) Sun-compass migration by *Aurelia aurita* (Scyphozoa): population retention and reproduction in Saanich Inlet, British Columbia. *Mar. Biol.*, **119**, 347–356.

Hamner, W. M. and Schneider, D. (1986) Regularly spaced rows of medusae in the Bering Sea: role of Langmuir circulation. *Limnol. Oceanogr.*, **31**, 171–177.

Katija, K. (2012) Biogenic inputs to ocean mixing. *J. Exp. Biol.*, **215**, 1040–1049.

Katija, K. and Dabiri, J. O. (2009) A viscosity-enhanced mechanism for biogenic ocean mixing. *Nature*, **460**, 624–626.

Kinsman, B. (1984) *Wind Waves*, Dover, New York.

Kunze, E., Dower, J. F., Beveridge, I., Dewey, R. and Bartlett, K. P. (2006) Observations of biologically generated turbulence in a coastal inlet. *Science*, **313**, 1768–1770.

Lai, Z., Chen, C., Beardsley, R., Rothschild, B. and Tian, R. (2010) Impact of high-frequency nonlinear internal waves on plankton dynamics in Massachusetts Bay. *J. Mar. Res.*, **68**, 259–281.

Larson, R. J. (1992) Riding Langmuir circulations and swimming in circles: a novel form of clustering behavior by the scyphomedusa *Linuche unguiculata*. *Mar. Biol.*, **112**, 229–235.

Leibovich, S. (1983) The form and dynamics of Langmuir circulations. *Ann. Rev. Fluid Mech.*, **15**, 391–427.

Lennert-Cody, C. E. and Franks, P. J. S. (1999) Plankton patchiness in high-frequency internal waves. *Mar. Ecol. Prog. Ser.*, **186**, 59–66.

Leshansky, A. M. and Pismen, L. M. (2010) Do small swimmers mix the ocean? *Phys. Rev. E*, **82**, 025301.

Macias, D., Somavilla, R., González-Gordillo, J. I. and Echevarría, F. (2010) Physical control of zooplankton distribution at the Strait of Gibraltar during an episode of internal wave generation. *Mar. Ecol. Prog. Ser.*, **408**, 79–95.

McHenry, M. and Jed, J. (2003) The ontogenetic scaling of hydrodynamics and swimming performance in jellyfish (*Aurelia Aurita*). *J. Exp. Biol.*, **206**, 4125–4137.

Miller, R. J. (1974) Distribution and biomass of an estuarine ctenophore population, *Mnemiopis leidyi* (*A. Agassiz*). *Chesapeake Sci.*, **15**, 1–8.

Downloaded from http://plankt.oxfordjournals.org/ by guest on February 1, 2016

Pauly, D., Graham, W., Libralato, S., Morissette, L. and Deng Palomares, M. L. (2009) Jellyfish in ecosystems, online databases, and ecosystem models. *Hydrobiologia*, **616**, 67–85.

Purcell, J. E. and Arai, M. N. (2001) Interactions of pelagic cnidarians and ctenophores with fish: a review. *Hydrobiologia*, **451**, 27–44.

Purcell, J. E., Brown, E. D., Stokesbury, K. D. E., Haldorson, L. H. and Shirley, T. C. (2000) Aggregations of the jellyfish Aurelia labiata: abundance, distribution, association with age-0 walleye pollock, and behaviors promoting aggregation in Prince William Sound, Alaska, USA. *Mar. Ecol. Prog. Ser.*, **195**, 145–158.

Rakow, K. C. and Graham, W. M. (2006) Orientation and swimming mechanics by the scyphomedusa *Aurelia* sp. in shear flow. *Limnol. Oceanogr.*, **51**, 1097–1106.

Shanks, A. L. and Graham, W. M. (1987) Orientated swimming in the jellyfish *Stomolopus meleagris* L. Agassiz (Scyphozoan: Rhizostomida). *J. Exp. Mar. Biol. Ecol.*, **108**, 159–169.

Stavn, R. (1971) The horizontal-vertical distribution hypothesis: Langmuir circulations and *Daphnia* distributions. *Limnol. Oceanogr.*, **16**, 453–466.

Uye, S., Fujii, N. and Takeoka, H. (2003) Unusual aggregations of the scyphomedusa Aurelia aurita in coastal waters along western Shikoku, Japan. *Plankton Biol. Ecol.*, **50**, 17–21.

Zaitsev, Y. P. (1992) Recent changes in the trophic structure of the Black Sea. *Fish. Oceanogr.*, **1**, 180–189.

Zorn, H. M., Churnside, J. H. and Oliver, C. W. (2000) Laser safety thresholds for cetaceans and pinnipeds. *Mar. Mamm. Sci.*, **16**, 186–200.

Downloaded from http://plankt.oxfordjournals.org/ by guest on February 1, 2016